Global Gravity Wave "Weather" in the Middle Atmosphere: Preliminary Insights from the CRISTA-SPAS Missions

Stephen D. Eckermann

E. O. Hulburt Center for Space Research, Code 7641.2, Naval Research Laboratory, Washington, DC 20375, USA
Phone: +1-202-404-1299
FAX: +1-202-404-8090
Email: eckerman@map.nrl.navy.mil

Peter Preusse, Bernd Schaeler, Jens Oberheide, Dirk Offerman

Department of Physics, University of Wuppertal, Gauss-Str. 20, D-42097 Wuppertal, Germany

Julio T. Bacmeister

Universities Space Research Association, 10227 Wincopin Circle, Suite #202, Columbia, MD, 21044, USA

Dave Broutman

Computational Physics, Inc., Suite #600, 2750 Prosperity Avenue, Fairfax, VA 22031, USA.

ABSTRACT

We describe a preliminary analysis of small-scale temperature perturbations in the stratosphere produced by long wavelength gravity waves, as measured globally during the CRISTA-SPAS missions. We focus on enhanced activity observed at the equator and near the southern tip of South America. Global ray-tracing simulations for the mission days indicate that the equatorial activity is broadly consistent with the transmission of nonzero phase speed waves into the stratosphere. Ray-tracing and mountain wave model simulations indicate that the activity over South America is produced by long wavelength mountain waves forced by flow over the Andes. The results suggest that study of global gravity wave "weather" in the middle atmosphere may soon be feasible.

1. INTRODUCTION

A range of weather-related phenomena in the lower atmosphere generates gravity waves. Examples include fronts (e.g., Eckermann *and* Vincent 1993), squall lines (Alexander *et al.* 1995), convective clouds (e.g., Alexander *and* Pfister 1995), cyclogenesis (e.g., Powers 1997), typhoons (e.g., Sato 1993), geostrophic adjustment of jet steams (e.g., Kaplan *et al.* 1997), flow over mountains (e.g., Ralph *et al.* 1993), and so on. If wind patterns aloft are favorable, some of these waves can propagate into the middle atmosphere. Due to decreasing atmospheric densities, gravity waves grow in amplitude with height and so must eventually generate instabilities and

Report Documentation Page

Form Approved
OMB No. 0704-0188

1. REPORT DATE	2. REPORT TYPE	3. DATES COVERED
2001		**00-00-2001 to 00-00-2001**

4. TITLE AND SUBTITLE	5a. CONTRACT NUMBER
Global Gravity Wave 'Weather' in the Middle Atmosphere: Preliminary Insights from the CRISTA-SPAS Missions	5b. GRANT NUMBER
	5c. PROGRAM ELEMENT NUMBER
6. AUTHOR(S)	5d. PROJECT NUMBER
	5e. TASK NUMBER
	5f. WORK UNIT NUMBER
7. PERFORMING ORGANIZATION NAME(S) AND ADDRESS(ES) **Naval Research Laboratory,E.O. Hulburt Center for Space Research,Washington,DC,20375**	8. PERFORMING ORGANIZATION REPORT NUMBER
9. SPONSORING/MONITORING AGENCY NAME(S) AND ADDRESS(ES)	10. SPONSOR/MONITOR'S ACRONYM(S)
	11. SPONSOR/MONITOR'S REPORT NUMBER(S)

12. DISTRIBUTION/AVAILABILITY STATEMENT
Approved for public release; distribution unlimited

13. SUPPLEMENTARY NOTES
Proceedings of the Solar Terrestrial and Space Physics Community, 13th. National Congress of the Australian Institute of Physics, ANARE Research Reports, Australian Antarctic Division, Kingston, Tasmania, R. J. Morris and P. J. Wilkinson eds., 146, 11-24, 2001.

14. ABSTRACT
see report

15. SUBJECT TERMS

16. SECURITY CLASSIFICATION OF:			17. LIMITATION OF ABSTRACT	18. NUMBER OF PAGES	19a. NAME OF RESPONSIBLE PERSON
a. REPORT	b. ABSTRACT	c. THIS PAGE			
unclassified	**unclassified**	**unclassified**	**Same as Report (SAR)**	**12**	

"break." Such quasi-continuous gravity wave breaking generates drag and diffusion that strongly influence the global circulation and temperature patterns of the middle atmosphere (e.g., Haynes *et al*. 1991; Fritts *and* Luo 1995; Alexander *and* Holton 1997).

While the impact of breaking gravity waves on the climatology of the middle atmosphere is well appreciated, far less is known about how shorter-term changes in weather-related gravity wave sources and local propagation environments affect the "weather" in the middle atmosphere. Such research has been stymied to date by a lack of data on the synoptic meteorology of the middle atmosphere and its contemporaneous gravity-wave activity. There have also been very few global models of gravity-wave production and propagation with any sort of forecasting capability.

These shortcomings in observations and modeling are slowly being resolved, allowing us to investigate "gravity wave weather" issues systematically for the first time. Next generation satellite instruments have sufficient spatial resolution to resolve explicitly large-scale gravity waves in the middle atmosphere (e.g., Ross *et al*. 1992; Fetzer *and* Gille 1994; Mende *et al*. 1994; Wu *and* Waters 1996; Dewan *et al.* 1998; Preusse *et al.* 1999; Eckermann *and* Preusse 1999). Similar advances in modeling have led to global models that can simulate and even forecast gravity wave activity generated by specific sources (e.g., Bacmeister *et al*. 1994; Marks *and* Eckermann 1995; Alexander *and* Holton 1997; Dörnbrack *et al.* 1998; Sato *et al*. 1999; Charron *and* Brunet 1999). This has enabled some initial comparisons between global models and global measurements of gravity waves in the middle atmosphere (Eckermann *and* Marks 1997; Alexander 1998; Eckermann *and* Preusse 1999).

We focus here on preliminary data from two observational campaigns with the CRISTA-SPAS satellite during shuttle missions STS-66 and STS-85 (November, 1994, and August, 1997, respectively). Analysis shows that large-scale gravity wave fluctuations are present in the stratospheric and mesospheric temperature measurements. These conclusions are buttressed by numerical models, which generate maps of gravity wave activity that resemble the measured fluctuations. These results provide some preliminary insights into the generation and filtering processes affecting gravity waves in the middle atmosphere.

2. THE CRISTA-SPAS MISSIONS

The Cryogenic Infrared Spectrometers and Telescopes for the Atmosphere (CRISTA) instrument operated aboard the Shuttle Pallet Satellite (SPAS) (Offermann *et al.* 1999). CRISTA-SPAS was deployed into orbit and later recovered by the shuttle during missions STS-66 (November 3-14, 1994) and STS-85 (August 7-16, 1997). Figure 1 shows deployment of CRISTA-SPAS by the orbiter's robot arm on November 4, 1994. Lee wave clouds downstream (west) of the Andean ridge over the Chubut River region in central Patagonia (Argentina) are visible in this photograph, indicating that mountain waves were being generated by flow over the Andes as CRISTA-SPAS was being prepared for orbit.

CRISTA is a limb-scanning instrument that measures infrared emission spectra with high spectral resolution (Riese *et al.* 1999; Grossmann 2000). Temperatures in the stratosphere and lower mesosphere are retrieved from the CO_2 Q-branch emission at 792 cm^{-1} (~12.6 μm). Full details of the "version 1" retrievals are given by Riese *et al.* (1999), which yielded temperatures with a precision ~1 K. The precision of the "version 2" data analyzed here is ~0.5 K. CRISTA uses two additional telescopes that look 18^o either side of the central telescope, corresponding to tangent heights separated by ~650 km. Each scanning telescope acquires a complete vertical profile every 200-400 km along track, depending on the measuring mode. These unique measurements yielded data with global coverage and high spatial resolution (see

Figure 2 of Riese *et al*. 1999). Mesospheric temperatures are retrieved from CO_2 emissions in the 652-657 cm^{-1} band, which are measured by the center telescope only. Their precision is estimated to be ~1 K. The vertical sampling interval is 1.5 km for both the stratospheric and mesospheric temperature data. Further details of the instrument and measurements are given by Offermann *et al.* (1999), Riese *et al*. (1999) and Grossmann (2000).

Figure 1: Astronaut photo of CRISTA-SPAS being deployed into orbit by the robot arm of the Space Shuttle Atlantis at 12:19 UT on 4th November, 1994. Visible below are lee wave clouds downstream of the southern Andes over the Chubut region of Argentina (~42°S). This photograph and others from STS-66 are accessible from NASA's shuttle image archive, at http://images.jsc.nasa.gov/iams/images/earth/STS066/html/20177512.htm.

Fetzer *and* Gille (1994, 1996) found large-scale gravity-wave fluctuations in stratospheric data acquired by the Limb Infrared Monitor of the Stratosphere (LIMS), which operated on the Nimbus 7 satellite during 1978-79. The precision and resolution of CRISTA measurements exceed those of LIMS. Furthermore, CRISTA measures spectra whereas LIMS was a filter instrument. This allows CRISTA to check the quality of the retrievals in regions of enhanced aerosol content (e.g., the tropical lower stratosphere). Retrieval modeling by Preusse *et al*. (1999) indicates that sinusoidal gravity wave temperature perturbations with wavelengths in excess of ~5 km vertically and ~200 km horizontally are resolved by the CRISTA temperature channels. Thus, gravity waves with wavelengths longer than these limits should be evident in the CRISTA temperature data.

To investigate this, we isolated small-scale temperature variability in the CRISTA temperature data. Synoptic variability was removed using a wavenumber 0-6 Kalman filter. Next, vertical profiles of residual fluctuations were analyzed using the Maximum Entropy Method (MEM) and harmonic analysis. MEM analysis was used to identify the energetic vertical wavelength oscillations in a given profile. These wavelengths were then used to constrain a harmonic fit over a 12 km altitude interval, which was progressively shifted over the full height range of the profile. In this way, two principal amplitudes and phases were determined as a function of height for each profile. Finally, a multiplier, determined by the instrument's "visibility" to this particular vertical wavelength, was used to scale the fitted amplitude. For further details, see Preusse *et al.* (1999) and Eckermann *and* Preusse (1999).

Figure 2 shows resulting global maps of small-scale temperature amplitudes at 20-30 km for 6 successive days during Mission 1 (STS-66). We note a band of enhanced variance at the equator that exhibits significant zonal asymmetry and day-to-day variability. This is

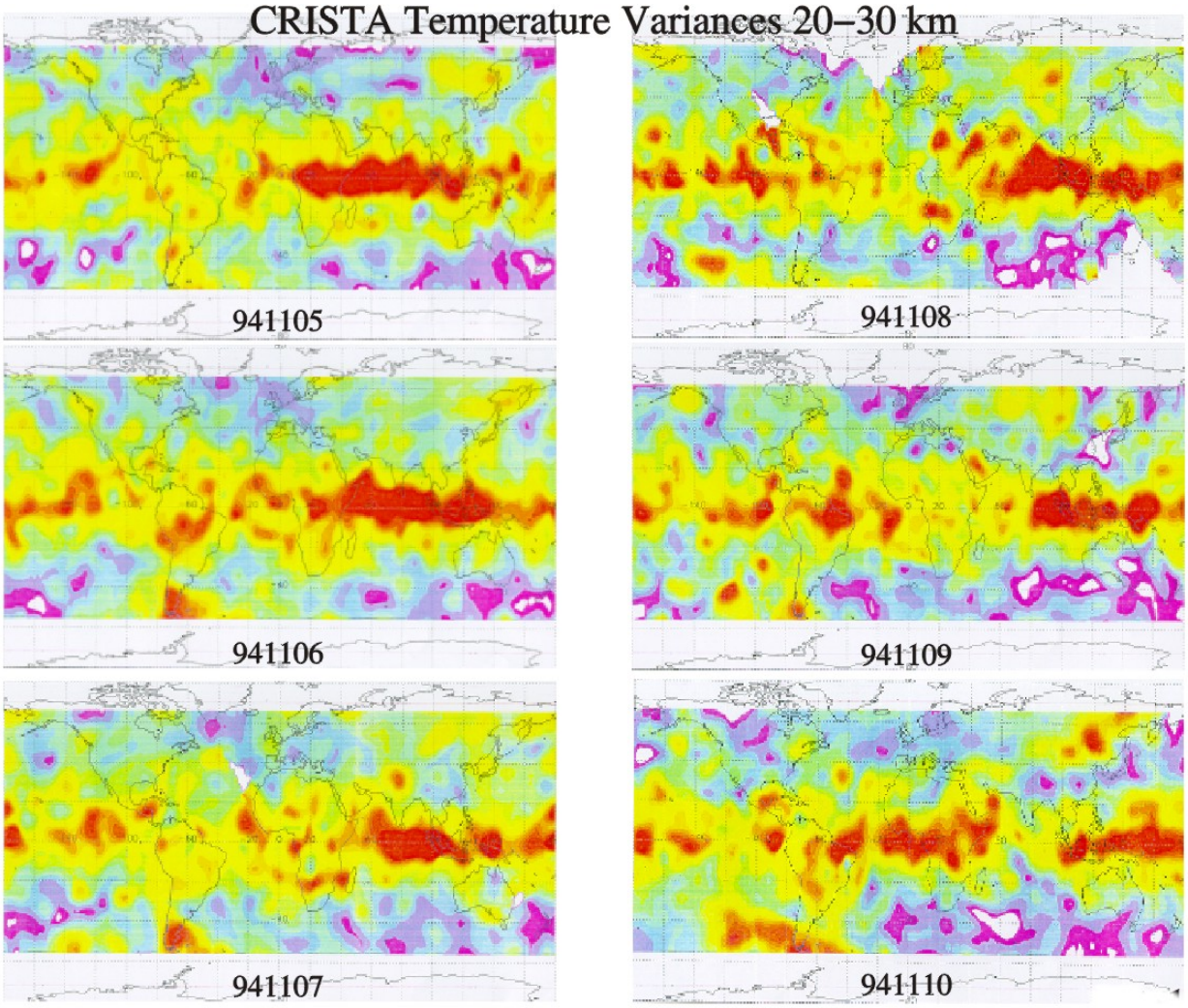

Figure 2: Preliminary global maps of CRISTA temperature amplitudes in the 20-30 km height range for six successive days during Mission 1 (5^{th}-10^{th} November, 1994). Red (dark) shading indicates highest values (~2.5 K), and blue-white shading shows smallest values.

superficially consistent with the notion of enhanced convective launching of gravity waves and equatorial waves into the tropical stratosphere (e.g., Alexander *and* Pfister 1995; Garcia 2000). We also note a persistent zone of enhanced activity near the southern tip of South America, consistent with the concept of mountain waves generated by flow over the southern Andes (see Figure 1) penetrating into the stratosphere. However, work by Alexander (1998) has demonstrated that straightforward interpretations of raw satellite gravity wave data such as these can be potentially misleading. Therefore we turn to global numerical modeling of gravity waves to make further progress in interpreting these and other features.

3. GLOBAL GRAVITY WAVE MODELS

3.1. *Gravity Wave Regional or Global Ray Tracer (GROGRAT)*

GROGRAT is a numerical model that uses ray-tracing techniques to track the propagation and amplitude evolution of nonhydrostatic gravity waves within arbitrary regional or global specifications of the Earth's atmosphere. Marks *and* Eckermann (1995) described the basic formulation of the model, while Eckermann *and* Marks (1997) reported subsequent

improvements and updates to the code. Further information can be found at the GROGRAT web site[1].

For the background atmosphere, we use 6 hourly global 2.5°x2° (144x91) wind and temperature data from NASA's Data Assimilation Office (DAO), which come gridded at 18 standard pressure levels from 1000 to 0.4 hPa (Schubert *et al.* 1993; Coy *and* Swinbank 1997). We resampled these data onto a 64x45x18 global grid. Comparison of Figures 3a and 3b shows that the major weather phenomena are retained in the wind fields after this resampling. GROGRAT absorbed these fields, first regridding them onto a geometrical height grid (using the DAO geopotential height fields), then fitting the data at each height with a superposition of spherical harmonics $Y_{m,n}(\varphi,\theta)$. Lower panels in Figure 3 show fits using spherical harmonics out to orders $(m,n)=(16,16)$ and $(m,n)=(32,32)$ (panels *c* and *d*, respectively). Both capture the overall structure quite well, but Figure 3d captures more of the finer-scale weather-related details in the winds. Thus, we used fits out to $(m,n)=(32,32)$ in our simulations. Note also that GROGRAT interpolates all the individual spherical harmonic coefficients at each fitting level with cubic splines, which ensures smoothly varying continuous derivatives in all three spatial directions.

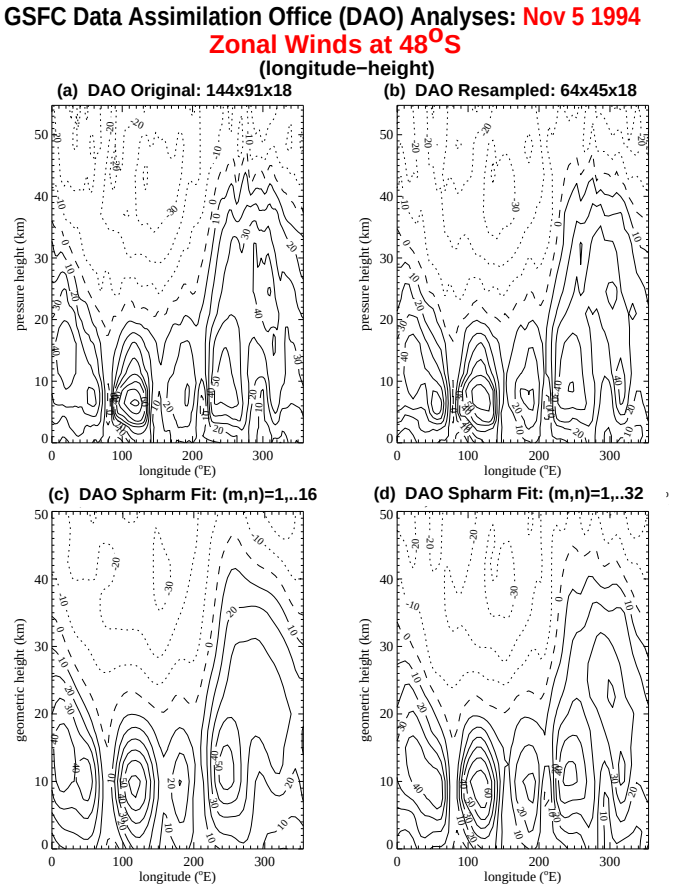

Figure 3: Longitude-height plot of DAO zonal wind at 48°S on 5th November, 1994 at 00:00 UT: (a) original data; (b) resampled to 64x45 in the horizontal; (c) after GROGRAT regridding to geometric heights and spherical harmonic fits to maximum $(m,n)=(16,16)$; (d) as for (c), but after spherical harmonic fits to maximum $(m,n)=(32,32)$. Contour labels are in m s^{-1}, positive values are eastward and have solid contour lines.

Here we ignore sources and concentrate on the transmission characteristics of the atmosphere. To this end, we used GROGRAT to trace a globally uniform distribution of waves through the middle atmosphere using DAO winds and temperatures during the mission days. Waves were launched at z_0 =1 km with ground-based phase speeds c = 0, 20 and 40 m s^{-1}, a horizontal wavelength λ_x = 50 km, a peak initial horizontal velocity amplitude of u' = 0.2 m s^{-1} and an isotropic distribution of 8 initial propagation directions. Wave amplitudes were controlled using a wave action conservation equation with damping terms due to turbulent diffusion, infrared radiative cooling and wave breaking/saturation (Marks *and* Eckermann 1995). A total of 13056 rays were traced over the globe.

Figure 4 shows global ray counts, weighted by the horizontal velocity amplitude of each ray, as a function of height on 6th November, 1994 at 00:00 UT. Results shown are for the c = 20 m s^{-1} waves, as might plausibly emanate from convection and other moving and/or evolving weather

[1] http://uap-www.nrl.navy.mil/dynamics/html/grograt.html

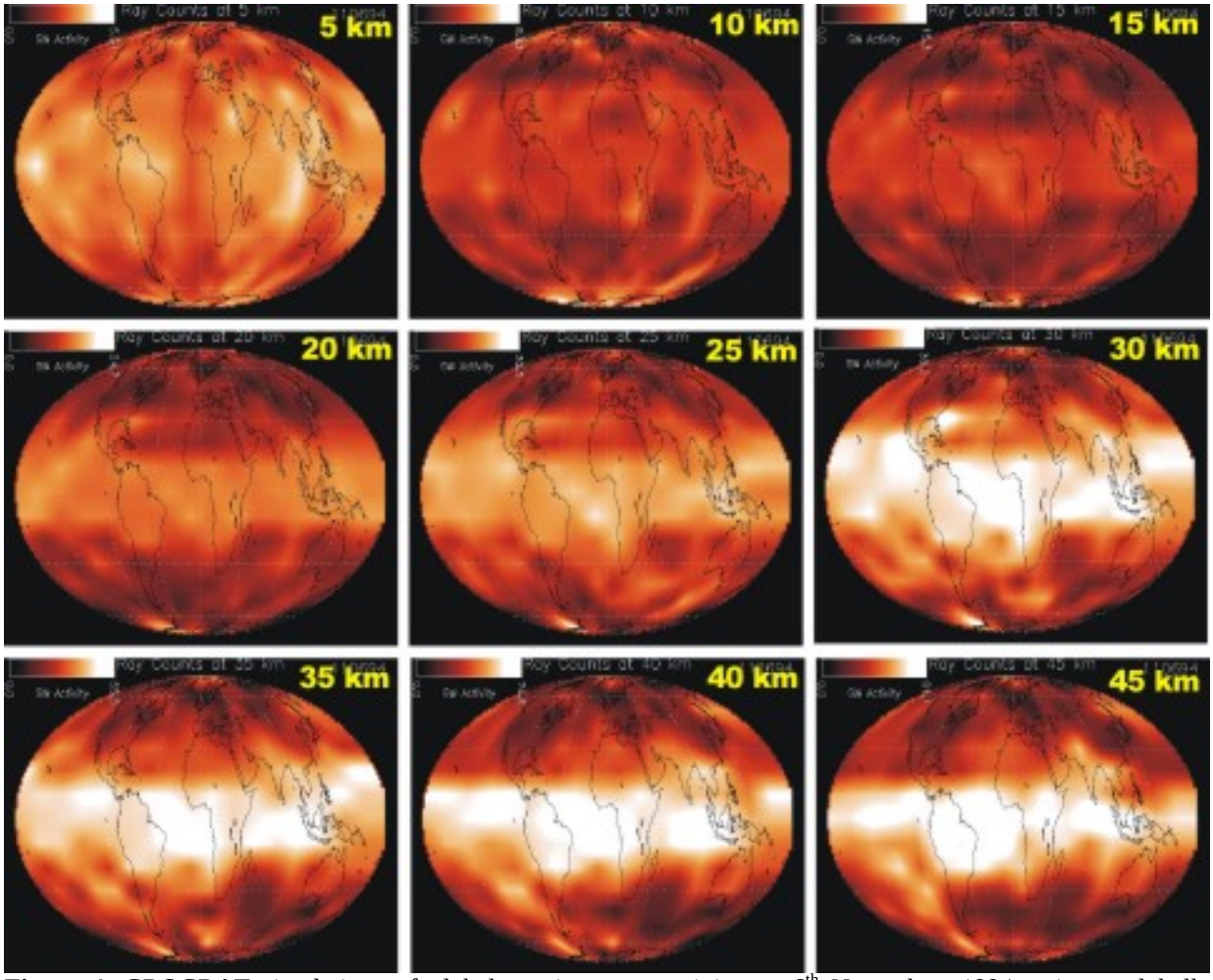

Figure 4: GROGRAT simulations of global gravity wave activity on 6th November, 1994, using a globally invariant source spectrum of waves of c=20 m s^{-1} (see text). Light values indicate large wave variances, darker values indicate small wave variances.

systems. Although wave amplitudes are globally uniform at z_0 =1 km, the variable background atmosphere quickly yields considerable geographical variability at upper heights. At z = 20 km and above, Figure 4 reveals a clear band of enhanced activity around the equator that resembles the enhanced equatorial activity at 20-30 km in the CRISTA data (Figure 2). It occurs in the model due to very light winds throughout the equatorial troposphere and stratosphere during Mission 1, which enables waves with nonzero phase speeds to propagate upwards without encountering critical layers or severe damping. However, the zonal asymmetry in Figure 2 is not reproduced in Figure 4, suggesting that zonally varying wave generation may also play a role in producing the observed activity.

We are investigating possible sources of equatorial wave activity during the missions. For example, during Mission 2 (STS-85; 7-16 August, 1997) similar bands of enhanced equatorial activity were observed. Super Typhoon Winnie developed over the South China Sea during the mission, reaching Category 5 ("super typhoon" status) on August 12 (see Figure 5). Typhoons are known to be strong sources of gravity waves (e.g., Matsumoto *and* Okamura 1985; Sato 1993), and thus Winnie might have produced enhanced stratospheric gravity wave activity. CRISTA used a "hawkeye" observational mode during Mission 2, which increased sampling over Indonesia but reduced overall coverage over the typhoon. Nevertheless, preliminary observations in this region show some suggestions of enhanced temperature

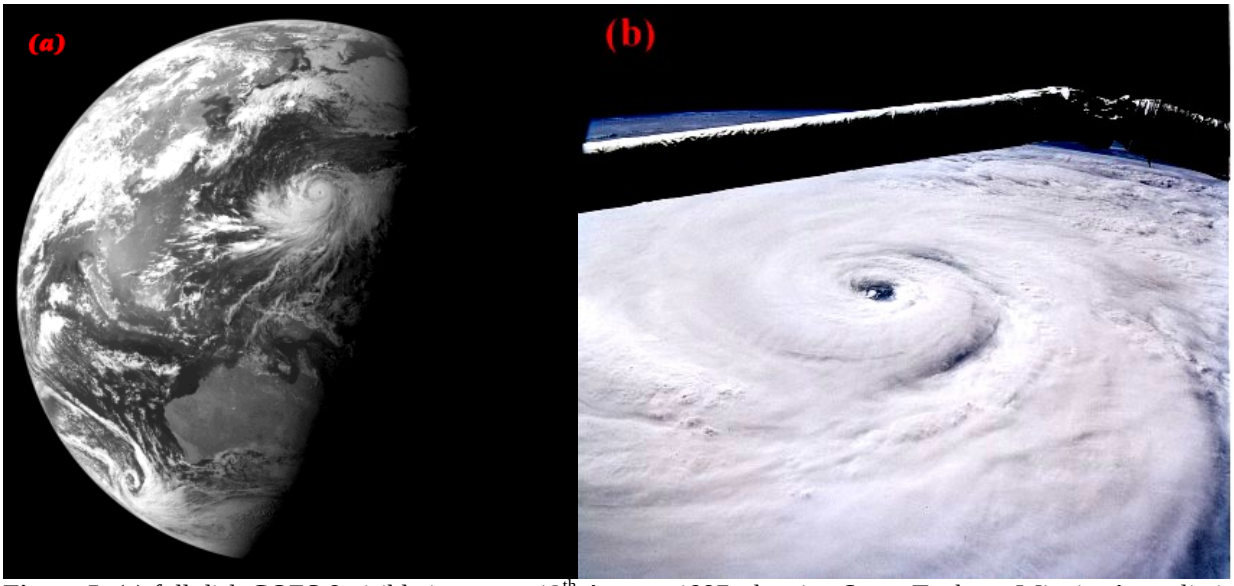

Figure 5: (a) full disk GOES 8 visible image on 12th August, 1997, showing Super Typhoon Winnie. Australia is visible to the south (image courtesy of NOAA's National Climatic Data Center); (b) close-up photo of Winnie taken from *Discovery* on 13th August (robot arm in foreground).

fluctuations in the stratosphere near the typhoon. Investigation of equatorial source processes continues.

3.2. *Naval Research Laboratory Mountain Wave Forecast Model (MWFM)*

Mountains are believed to be a strong extratropical source of gravity waves for the middle atmosphere (Nastrom *and* Fritts 1992; Bacmeister 1993). With this in mind, the Naval Research Laboratory Mountain Wave Forecast Model (MWFM) was developed to forecast the turbulence produced by breaking mountain waves in the stratosphere, as an aid to safe flight planning for NASA's stratospheric ER-2 research aircraft (Bacmeister *et al.* 1994; Eckermann *et al.* 2000). The model uses a database of quasi-two-dimensional ridges inferred from high-resolution digital topography. Surface winds from forecast data are blown across these ridges and used to generate waves. Wave equations are used thereafter to trace any vertical extension of this activity into the atmosphere, as well as any subsequent wave breaking. Further information can be found at the MWFM web site[2].

Here we use the MWFM with DAO data to generate an initial global field of mountain waves forced at the ground. We use GROGRAT thereafter to track the propagation of these waves to greater heights, using fitted DAO data as before. Figure 6 shows modeled mountain wave activity at z = 25 km from 5-10 November, 1994. We note that stratospheric mountain wave activity is predicted at the southern tip of South America during Mission 1, which resembles the activity observed by CRISTA in Figure 2. However, there is additional activity over Eurasia and western North America in Figure 6 that is not seen as clearly in Figure 2.

In analyzing MLS radiance fluctuations, Alexander (1998) stressed the importance of accounting for the spatial filtering of the satellite gravity wave measurement. Mountain wave vertical wavelengths are given approximately by

[2] http://uap-www.nrl.navy.mil/dynamics/html/mwfm.html

$$\lambda_z = \frac{2\pi U \cos\varphi}{N} \qquad (1)$$

where U is the horizontal wind speed, N is the Brunt-Väisälä frequency and φ is the angle between the horizontal wind and wave vectors. Between 40°–50°S over South America (~70°W) the DAO winds blow approximately orthogonal to the Andean ridge axis, implying $\varphi \sim 0°$. At

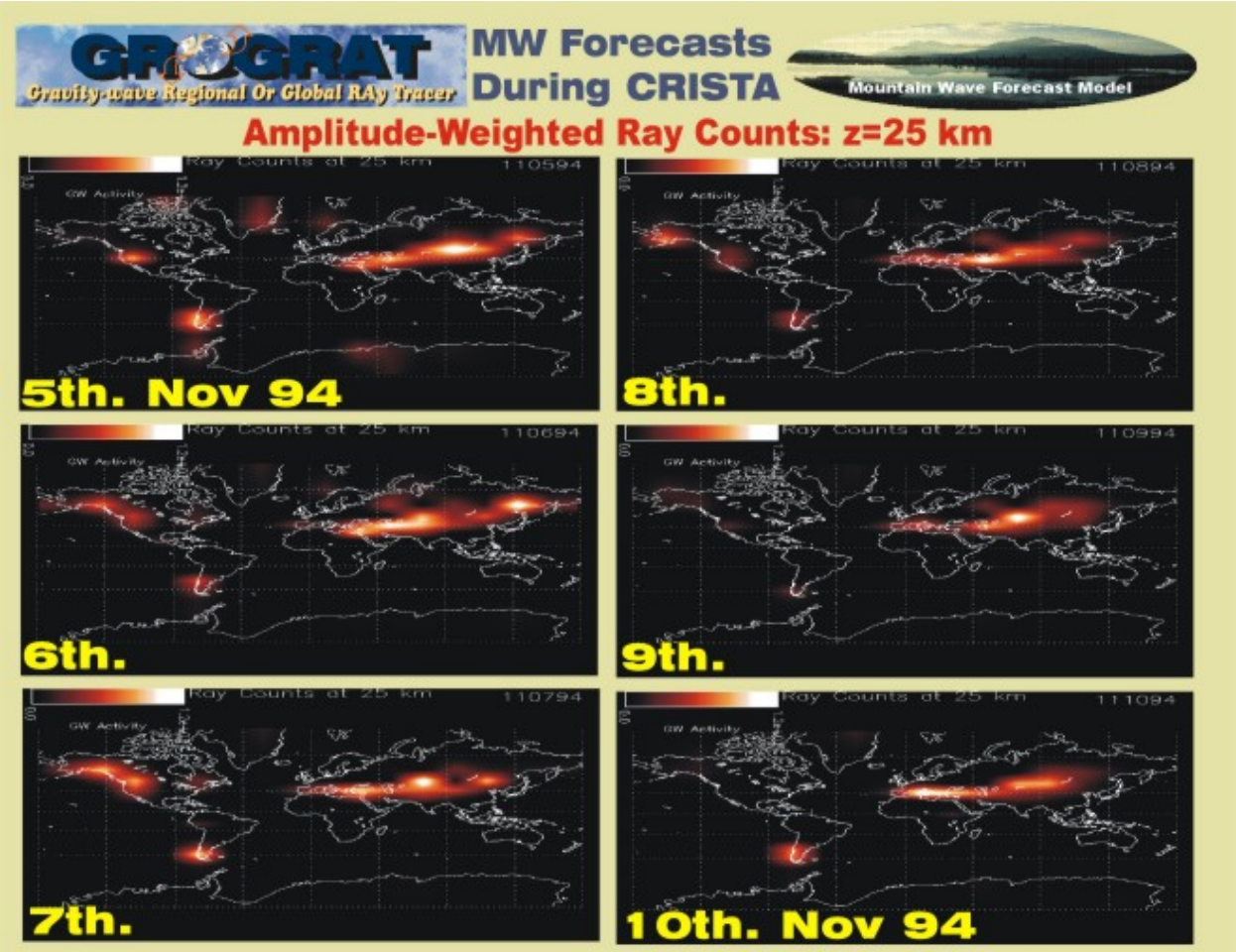

Figure 6: Coupled GROGRAT-MWFM simulations of global mountain wave amplitudes at z = 25 km, using DAO winds and temperatures. Light (dark) values depict large (small) wave activity.

20-30 km, U ~20-50 m s^{-1} (see Figure 3) and N ~ 0.02 rad s^{-1}, yielding λ_z ~ 6-16 km from (1). Conversely, U ~10 m s^{-1} at 30°N, yielding vertical wavelengths no greater than ~3 km here. Since CRISTA is sensitive to vertical wavelengths λ_z > 5 km, it can resolve the long λ_z waves over South America but not the shorter λ_z waves at northern latitudes.

To assess this quantitatively, Figure 7 shows the model results from Figure 6 after imposition of a filter which retains only those waves with vertical wavelengths λ_z > 10 km. We see that the activity over southern South America is now more prominent and activity in the Northern Hemisphere is significantly attenuated, which is more in line with the data in Figure 2. Alexander (1998) reported similarly improvements on comparing filtered model data to the MLS radiance fluctuations reported by Wu *and* Waters (1996).

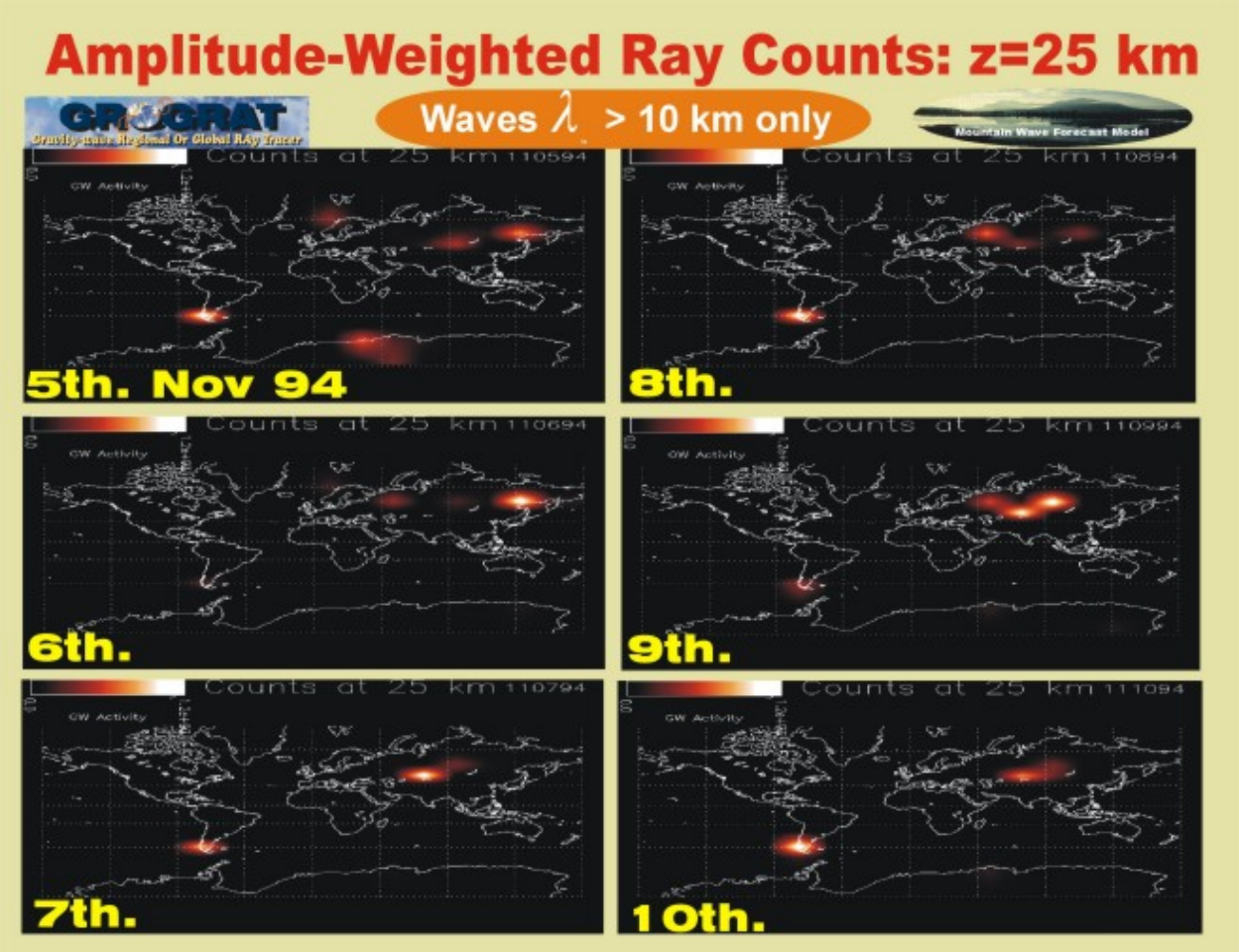

Figure 7: As in Figure 6, but after imposition of a filter which retains λ_z > 10 km waves only.

Eckermann *and* Preusse (1999) present an in-depth study of temperature fluctuations observed by CRISTA over southern South America and central Eurasia. Using simple mountain wave theory and "next generation" MWFM hindcast simulations, they show conclusively that this activity is produced by long wavelength mountain waves which propagate into the stratosphere. Mesoscale modeling work by Tan *and* Eckermann (2000) generates stratospheric mountain waves very similar to those measured by CRISTA over the southern Andes on 6th. November, 1994.

4. SUMMARY

Initial comparisons between the small-scale temperature perturbations measured by CRISTA (Figure 2) and global gravity wave model predictions are encouragingly favorable. These findings further support the conclusion that CRISTA temperature measurements in the stratosphere and mesosphere resolved large-scale gravity waves (see also Preusse *et al.* 1999; Eckermann *and* Preusse 1999). Global synoptic data on gravity waves in the middle atmosphere are still very limited, having been inferred from a few earlier satellite measurements only (Fetzer *and* Gille 1994 1996; Wu *and* Waters 1996). Furthermore, interpretation of some of these earlier measurements has not always been straightforward (Alexander 1998). Yet global measurements of gravity waves and accompanying theoretical explanations of the observed features are vital to a proper understanding of the "weather" in the middle atmosphere, which is very sensitive to gravity wave driving from below. Our analysis suggests that some key features

in the CRISTA data are consistent with specific gravity wave production and filtering processes. Further analysis and modeling of these data are being pursued.

ACKNOWLEDGEMENTS

This research was supported in part by the Office of Naval Research and by NASA through grants NAS5-98045 and L68786D. Thanks to Iain Reid for the invitation and support to attend the AIP conference and the University of Adelaide.

REFERENCES

Alexander, M. J. (1998). Interpretations of observed climatological patterns in stratospheric gravity wave variance, *Journal of Geophysical Research 103*: 8627-8640.

Alexander, M. J. *and* Holton, J. R. (1997). A model study of the zonal forcing in the equatorial stratosphere by convectively induced gravity waves, *Journal of the Atmospheric Sciences 54*: 1408-419.

Alexander, M. J. *and* Pfister, L. (1995). Gravity wave momentum flux in the lower stratosphere over convection, *Geophysical Research Letters 22*: 2029-2032.

Alexander, M. J., Holton, J. R. *and* Durran, D. R. (1995). The gravity wave response above deep convection in a squall line simulation, *Journal of the Atmospheric Sciences 52*: 2212-2226.

Bacmeister, J. T. (1993). Mountain-wave drag in the stratosphere and mesosphere inferred from observed winds and a simple mountain-wave parameterization scheme, *Journal of the Atmospheric Sciences 50*: 377-399.

Bacmeister, J. T., Newman, P. A., Gary, B. L. *and* Chan, K. R. (1994). An algorithm for forecasting mountain wave-related turbulence in the stratosphere, *Weather and Forecasting 9*: 241-253.

Charron, M., *and* Brunet, G. (1999). Gravity wave diagnosis using empirical normal modes, *Journal of the Atmospheric Sciences 56*: 2706-2727.

Coy, L. *and* Swinbank, R. (1997). Characteristics of stratospheric winds and temperatures produced by data assimilation, *Journal of Geophysical Research 102*: 25,763-25,781.

Dewan, E. M., Picard, R. H., O'Neil, R. R., Gardiner, H. A., Gibson, J., Mill, J. D., Richards, E., Kendra, M., *and* Gallery, W. O. (1998). MSX satellite observations of thunderstorm-generated gravity waves in mid-wave infrared images of the upper stratosphere, *Geophysical Research Letters 25*: 939-942.

Dörnbrack, A., Leutbecher, M., Volkert, H. *and* Wirth, M. (1998). Mesoscale forecasts of stratospheric mountain waves, *Meteorol. Appl. 5*: 117-126.

Eckermann, S. D., *and* Marks, C. J. (1997). GROGRAT: A new model of the global propagation and dissipation of atmospheric gravity waves, *Advances in Space Research 20(6)*: 1253-1256.

Eckermann, S. D. *and* Preusse, P. (1999). Global measurements of stratospheric mountain waves from space, *Science 286*: 1534-1537.

Eckermann, S. D. *and* Vincent, R. A. (1993). VHF radar observations of gravity-wave production by cold fronts over southern Australia, *Journal of the Atmospheric Sciences 50*: 785-806.

Eckermann, S. D., Broutman, D., Tan, K. A., Preusse, P. *and* Bacmeister, J. T. (2000). Mountain waves in the stratosphere, *NRL Review,* in press.

Fetzer, E. J. *and* Gille, J. C. (1994). Gravity wave variance in LIMS temperatures. Part I: variability and comparison with background winds, *Journal of the Atmospheric Sciences 51*: 2461-2483.

Fetzer, E. J. *and* Gille, J. C. (1996). Gravity wave variance in LIMS temperatures. Part II: comparison with the zonal-mean momentum balance, *Journal of the Atmospheric Sciences 53*: 398-410.

Fritts, D. C. *and* Luo, Z. (1995) Dynamical and radiative forcing of the summer mesopause circulation and thermal structure, 1, mean solstice conditions, *Journal of Geophysical Research 100*: 3119-3128.

Garcia, R. R. (2000). The role of equatorial waves in the semiannual oscillation of the middle atmosphere, in *Atmospheric Science Across the Stratopause*, American Geophysical Union Monograph Series, D. E. Siskind, M. E. Summers and S. D. Eckermann editors, in press.

Grossmann, K. U. (2000). Recent improvements in middle atmosphere remote sounding techniques: the CRISTA-SPAS experiment, in *Atmospheric Science Across the Stratopause*, American Geophysical Union Monograph Series, D. E. Siskind, M. E. Summers and S. D. Eckermann editors, in press.

Haynes, P. H., Marks, C. J., McIntyre, M. E., Shepherd, T. G. *and* Shine, K. P. (1991). On the "downward control" of extratropical diabatic circulations by eddy-induced mean forces, *Journal of the Atmospheric Sciences 48*: 651-678.

Kaplan, M. L., Koch, S. E., Lin, Y.-L., Weglarz, R. P. *and* Rozumalski, R. A. (1997). Numerical simulations of a gravity wave event over CCOPE, I, the role of geostrophic adjustment in mesoscale jetlet formation, *Monthly Weather Review 125*: 1185-1211.

Marks, C. J. *and* Eckermann, S. D. (1995). A three-dimensional nonhydrostatic ray-tracing model for gravity waves: formulation and preliminary results for the middle atmosphere, *Journal of the Atmospheric Sciences 52*: 1959-1984.

Matsumoto, S. *and* Okamura, H. (1985). The internal gravity wave observed in the Typhoon T8124 (Gay), *Journal of the Meteorological Society of Japan 63*: 37-51.

Mende, S. B., Swenson, G. R., Geller, S. P., *a*nd Spear, K. A. (1994). Topside observations of gravity waves, *Geophysical Research Letters 21*: 2283-2286.

Nastrom, G. D. *and* Fritts, D. C. (1992). Sources of mesoscale variability of gravity waves, 1, topographic excitation, *Journal of the Atmospheric Sciences 49*: 101-110.

Offermann, D., Grossmann, K. U., Barthol, P., Knieling, P., Riese, M. *and* Trant, R. (1999). The Cryogenic Infrared Spectrometers and Telescopes for the Atmosphere (CRISTA) experiment and middle atmosphere variability, *Journal of Geophysical Research 104*: 16,311-16,325.

Powers, J. G. (1997). Numerical model simulations of a mesoscale gravity wave event: sensitivity tests and spectral analysis, *Monthly Weather Review 125*: 1838-1869.

Preusse, P., Schaeler, B., Bacmeister, J. T. *and* Offermann, D. (1999). Evidence for gravity waves in CRISTA temperatures, *Advances in Space Research* (in press).

Ralph, F. M., Neiman, P. J., *and* Levinson, D. (1993). Lidar observations of a breaking mountain wave associated with extreme turbulence, *Geophysical Research Letters 24*: 663-666.

Riese, M., Spang, R., Preusse, P., Ern, M., Jarisch, M., Offerman, D. *and* Grossman, K. U. (1999). Cryogenic Infrared Spectrometers and Telescopes for the Atmosphere (CRISTA) data processing and atmospheric temperature and trace gas retrieval, *Journal of Geophysical Research 104*: 16,349-16,367.

Ross, M. N., Christensen, A. B., Meng, C.-I., *and* Carbary J. F. (1992). Structure in the UV nightglow observed from low Earth orbit, *Geophysical Research Letters 19*: 985-988.

Sato, K. (1993). Small-scale wind disturbances observed by the MU radar during the passage of Typhoon Kelly, *Journal of the Atmospheric Sciences 50*: 518-537.

Sato, K., Kumakura, T. *and* Takahashi, M. (1999). Gravity waves appearing in a high-resolution GCM simulation, *Journal of the Atmospheric Sciences 56*: 1005-1018.

Schubert, S. D., Rood, R. B. *and* Pfaendtner, J. (1993). An assimilated dataset for Earth science applications, *Bulletin of the American Meteorological Society 74*: 2331-2342.

Tan, K. A. *and* Eckermann, S. D. (2000). Numerical model simulations of mountain waves in the middle atmosphere over the southern Andes, in *Atmospheric Science Across the Stratopause*, American Geophysical Union Monograph Series, D. E. Siskind, M. E. Summers and S. D. Eckermann editors, in press.

Wu, D. L. *and* Waters, J. W. (1996). Gravity-wave-scale temperature fluctuations seen by the UARS MLS, *Geophysical Research Letters 23*: 3289-3292.